

Development of a Digital Micropump with Controlled Flow Rate for Microfluidic Platforms

Mohammad Paknahad, Hojatollah Rezaei Nejad, * Mina Hoorfar

^{1, 2, 3} University of British Columbia, School of Engineering,
3333 University Way, Kelowna, BC V1V1V7, Canada

* Tel.: 1-250-807-8804, Fax: 1-250-8-7-9850

* E-mail: mina.hoorfar@ubc.ca

Received: 31 October 2014 /Accepted: 1 December 2014 /Published: 31 December 2014

Abstract: This paper presents a novel device for pumping a column of liquid in a microchannel integrated on a digital microfluidic (DMF) platform. The electrowetting on dielectric (EWOD) method is used to frequently actuate a droplet (referred to as the piston droplet) on an array of electrodes. A column of liquid (referred to as the pumped droplet) is pumped in a microfluidic channel by the pressure coming from actuation of the piston droplet. A signal modulation technique is developed and used in order to control the flow rate of the liquid column in the microchannel. Different flow rates of the pumped liquid are achieved by controlling the actuation time of the signal used for moving the piston droplet. Copyright © 2014 IFSA Publishing, S. L.

Keywords: Digital microfluidics (DMF), Droplet manipulation, Electrowetting on dielectric (EWOD), SU8-based microchannel, 3D-printed microchannel, Micropump.

1. Introduction

Recent efforts have focused on replacing the conventional macro-systems with lab-on-chip (LOC) systems to enhance transport, reaction and manipulation of different fluid samples [1]. The first generations of LOC systems include microchannels for flowing fluid [2]. These systems referred to as continuous microfluidics require peripheral devices such as micropumps and microvalves. Continuous microfluidics is a well-established platform used to process and analysis biofluids in different applications [3]. Over the past decades, a variety of detection methods have also been developed and integrated into continuous microfluidic platforms [4-6]. Despite the general success of these platforms, it is required to use external elements and moving parts to manipulate the fluids in microchannels. This can hinder portability and

integrability of the continuous platforms for in-field applications.

Digital microfluidics (DMF), a relatively new type of microfluidic systems working based on manipulation of individual droplets on planar electrode arrays, has been used to perform different fluidic operation in micron scales [7-8]. For its unique advantages (including the reduced sample size, rapid analysis, ease of fabrication, portability, and low cost [7-9]), DMF has shown a great potential to perform conventional bio-chemical laboratory operations ranging from DNA purification to cell culture and single cell analysis [10].

To take advantage of the features of both platforms, the integration of continuous and DMF systems has attracted attentions [7-9]. This paper presents a novel technique to manipulate a column of liquid in microchannels on a DMF platform. For this purpose, an array of electrodes is fabricated on a

glass substrate covered with dielectric and hydrophobic layers. To integrate a microchannel on the DMF platform, two different techniques has been used:

i) Two thin walls of SU8 are fabricated on two sides of electrodes and a top plate is mounted on top of the SU8 walls [11], and

ii) A 3D printed microchannel is integrated with the top and bottom plates of the DMF platform (all three parts are held together by the clamping force). An array of electrodes is used to actuate a droplet in the microchannel. It is shown that the fabricated device is capable of pumping a column of liquid in the microchannel. In essence, a target droplet (referred to as the pumped droplet) is pumped by actuating the secondary droplet (referred to as the piston droplet) in a microfluidic channel using the electrowetting on dielectric (EWOD) method. To control the flow rate of the liquid column in the microchannel, a signal modulation technique is developed and utilized. Different flow rates of the pumped liquid are achieved by controlling the actuation signal of the piston droplet.

2. Experimental Setup

The schematic diagram of the experimental setup is depicted in Fig. 1a. A signal generator is used to create an AC square wave signal. A voltage amplifier is used to amplify the output of the signal generator. The high voltage signal from the amplifier output is then sent to an interface circuit designed to switch the signal on and off by the operator. The modulated high-voltage output signal from the interface circuit is used to drive the DMF platform. The details of the interface circuit are shown in Fig. 1b.

3. Fabrication Process

Integration of a microchannel on a DMF platform is achieved by two different methods. In the first method, a series of electrodes on a copper-coated glass substrate is patterned using the S1805 positive photoresist and the standard photolithography technique (see Fig. 2). Each of electrodes has a surface area of $1.5\text{ mm} \times 1.5\text{ mm}$. To create the sidewalls of the channel, the SU8 negative photoresist is spin-coated on the chip, and then the mask with a straight-channel pattern is aligned on the chip and exposed to the UV light. The process is followed by developing the SU8 layer in the developer solution. The S1813 positive photoresist is spun on the chip as a dielectric layer. An ITO glass is used as the top plate. To make the device hydrophobic, both bottom and top plates are coated by a thin layer of Teflon. The top plate is utilized for sealing the channel and providing the ground electrode for the DMF electrodes. The channel height using this method is around $100\text{ }\mu\text{m}$.

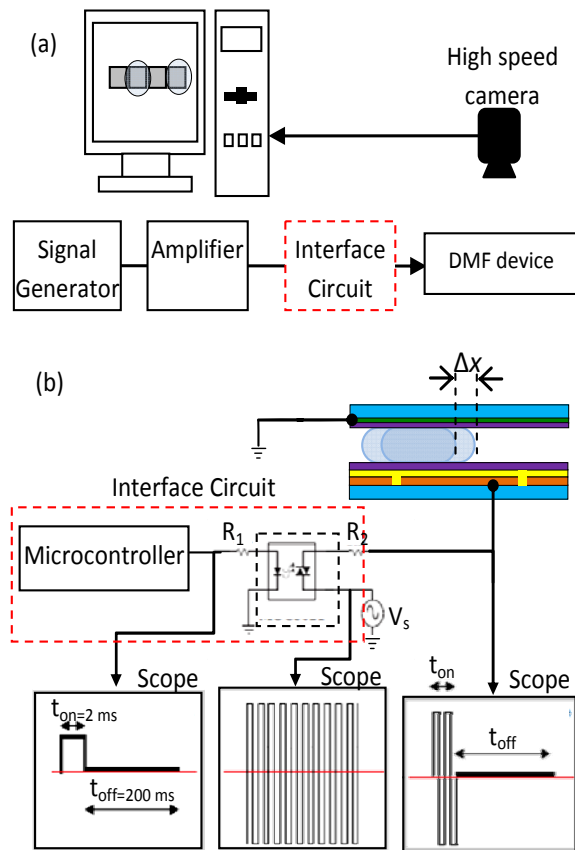


Fig. 1. a) Schematic of the experimental setup, and b) the interface circuit designed for modulation of the applied AC signal and integration into the DMF platform.

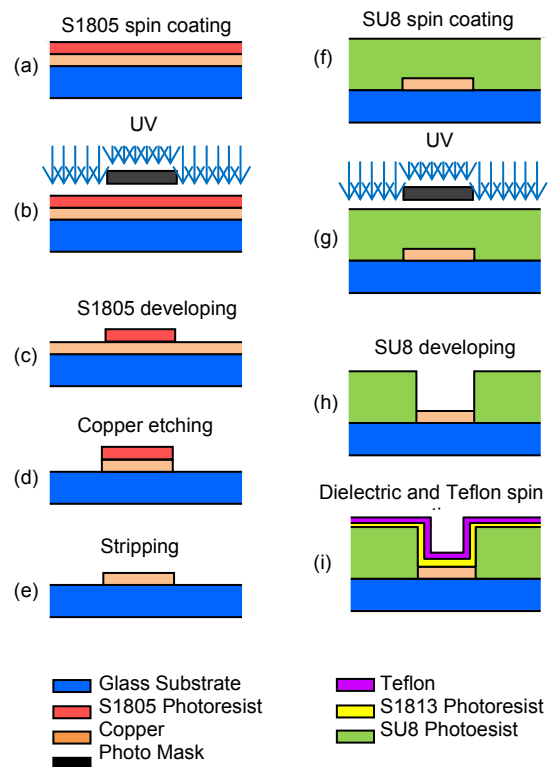


Fig. 2. Fabrication process and integration of a SU8-based microchannel on a DMF platform.

To create a microchannel with a larger depth, another method of fabrication is introduced using a 3D-printed frame. The thickness of the frame (i.e. the gap size between the bottom and top plates) is 200 μm , and the channel width is considered to be equal to the width of the fabricated DMF electrodes (1.5 mm). The frame is designed in a way to hold the bottom and top plates in a desired position. The schematic of the 3D-printed frame and its final integration with the top and bottom plates are shown in Fig. 3 (a) and Fig. 3 (b), respectively. Since the 3D-printed frame deforms in the temperature above 60 $^{\circ}\text{C}$, it was not possible to make it hydrophobic using Teflon coating. Thus, the microchannel was treated by the NeverWetTM Repelling spray (from Rust-Oleum) to reduce droplet adhesion to the 3-D printed frame.

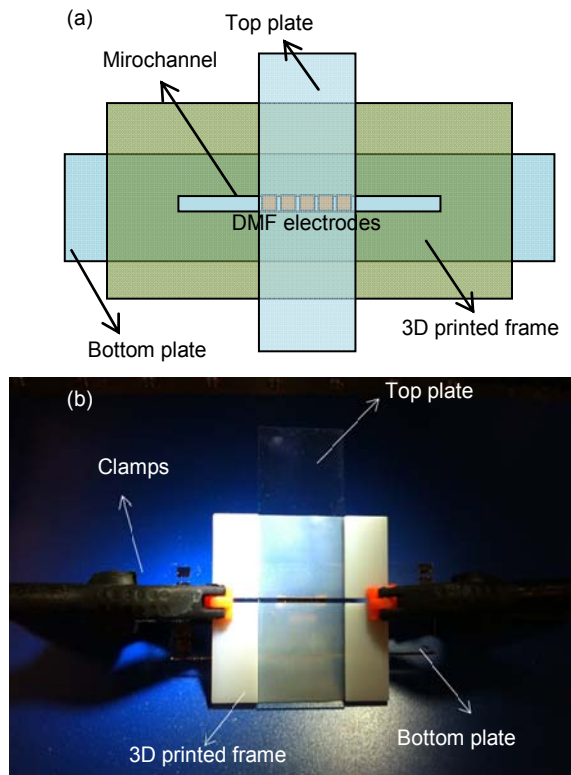


Fig. 3. (a) Schematic of the 3D-printed frame, and (b) 3D-printed microchannel integrated with the top and bottom plates. The clamps are applied to the assembly to squeeze the droplet between the bottom plate and top plates.

4. Experimental Procedure

For all the experiments, two deionized (DI) water droplets with the distance of 5 mm are dispensed on the array of electrodes on the bottom plate. The top plate is placed on the top of the droplets over either the pair of the SU8 sidewalls or the 3D-printed frame. The volume of the piston droplet used for the experiments is 0.45 μL . The pumped liquid volume is chosen as 0.65 μL . Silicon oil is used as the filler medium to reduce friction and improve sealing of the

channel. The pumped droplet is actuated with the signal coming from the designed interface circuit (Fig. 1 (b)). In essence, the actuation signal of the piston droplet is precisely controlled to create the desired transport rate for the pumped droplet. As it is shown in Fig. 1, the signal coming from the amplifier output is an AC square wave. Using the interface circuit, this signal is frequently switched on and off for periods of t_{on} and t_{off} , respectively. The interface circuit output AC signal is applied to the electrode beneath the piston droplet. This way, the droplet is manipulated for the controlled period of time (t_{on}).

5. Theory

A theoretical model is developed to calculate the pressure generated in the microchannel by the piston droplet. The equivalent electrical circuit for droplet actuation by electrowetting on dielectric (EWOD) is shown in Fig. 4. Here, C_L and R_L are the capacitance and the resistance of the piston droplet, respectively. C_O and C_D are the capacitance of the oil on the energized electrode and the capacitance of the dielectric layer, respectively.

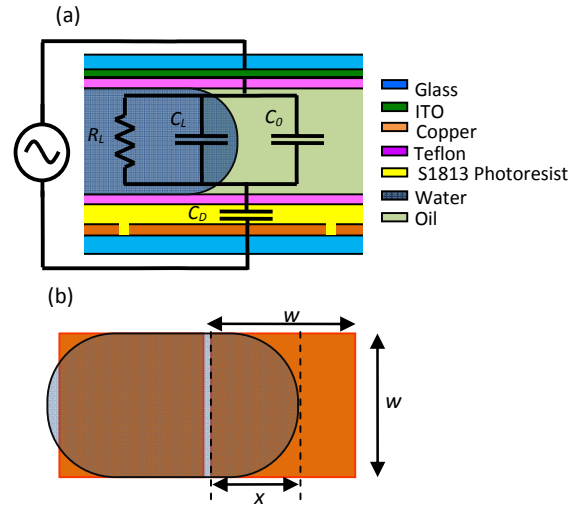


Fig. 4. (a) A schematic of the equivalent electrical circuit that models the droplet actuation mechanism based on the electrowetting-on-dielectric (EWOD) technique, (b) droplet actuation on copper electrodes (top view).

The total impedance of the system can be calculated as

$$Z_{\text{total}} = \frac{1}{\frac{1}{R_L} + (C_O + C_L)i\omega} + \frac{1}{i\omega C_D}, \quad (1)$$

where ω is the frequency of the applied field, and $i = \sqrt{-1}$. The capacitance and resistance values can be found based on physical and geometrical characteristics of the droplet and the DMF system.

$$\begin{cases} A = w^2 \\ R_L = \frac{\rho \cdot d}{A} \\ C_L = \frac{\epsilon_0 \epsilon_L w \cdot x}{d} \\ C_D = \frac{\epsilon_0 \epsilon_D \cdot A}{t} \\ C_o = \frac{\epsilon_0 \epsilon_o \cdot (A - w \cdot x)}{d} \end{cases} \quad (2)$$

In the above relations, p , d and w are the electrical resistivity of the droplet, the gap between the bottom and top plates (i.e., the height of the microchannel), and the width of the electrode (or the width of the microchannel), respectively. ϵ_L , ϵ_D , and ϵ_o are the relative permittivity of the liquid droplet, the dielectric layer, and oil medium, respectively. Here, x represents the length of the portion of the energized electrode covered with the droplet (see Fig. 4(b)).

In this study, the DI water droplet used as the piston droplet has the resistivity value of approximately $11 \text{ M}\Omega\text{cm}$. Therefore, the resistance of the piston droplet can be assumed very large, and hence Equation (1) can be simplified to

$$Z_{eq} = \frac{1}{i\omega C_{eq}} \quad (3)$$

where C_{eq} is the equivalent capacitance of the system and can be written as

$$C_{eq} = \frac{C_D(C_o + C_L)}{C_o + C_L + C_D} \quad (4)$$

By considering Equation (2), the equivalent capacitance of the system will be

$$C_{eq} = \frac{\epsilon_0 \epsilon_D w^2 (\epsilon_o w + (\epsilon_L - \epsilon_o) x)}{\epsilon_o t w + \epsilon_D w d + (\epsilon_L - \epsilon_o) t x} \quad (5)$$

The energy that is stored in the system based on the equivalent capacitance of the system can be calculated as

$$E = \frac{1}{2} C_{eq} \cdot V_{rms}^2 \quad (6)$$

Therefore, the derivative of the energy of the system with respect to the position of the droplet on the actuated electrode presents the electrowetting force that drives the piston droplet (see Equation (7)).

$$F_{electrowetting} = \frac{dE}{dx} = \frac{1}{2} V_{rms}^2 \frac{dC_{eq}}{dx} \quad (7)$$

Fig. 5 presents the energy stored in the system and the electrowetting (presented as the slope of the line fitted to the results) calculated based on Equation (7) for both cases of the SU8-based and 3D-printed microchannels. It is found that the energy stored in the system is linearly proportional to the position of the droplet on the actuated electrode, and the electrowetting force applied on the piston droplet (dE/dx) is equal to $70 \text{ }\mu\text{N}$ for the $100\text{-}\mu\text{m}$ -high SU8 microchannel and $50 \text{ }\mu\text{N}$ for $200\text{-}\mu\text{m}$ -high 3D-printed microchannel. The pressure generated in the microchannel by the piston droplet can be found by dividing the electrowetting force by the cross sectional area of the channel ($d \times w$, where d and w present the height and width of the channel, respectively). The pressure caused by actuating the pumped droplet is estimated to be 467 Pa for the $100\text{-}\mu\text{m}$ -high SU8-based microchannel and 166.7 Pa for the $200\text{-}\mu\text{m}$ -high 3D-printed microchannel.

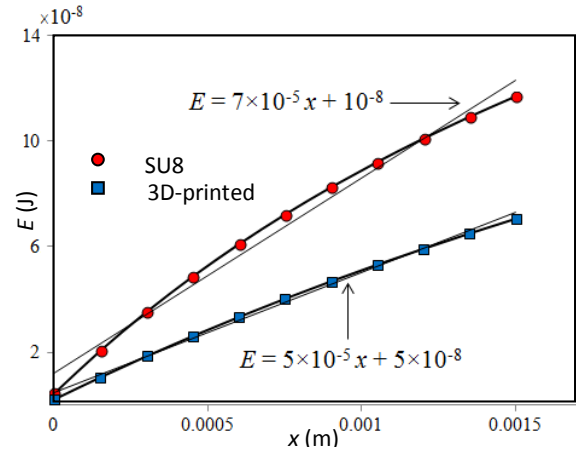


Fig. 5. The red circle and the blue square symbols show the energy stored in the system calculated from Equation (7) for the SU8-based and the 3D-printed microchannels, respectively. The slopes of the black solid lines fitted by linear regression to each set of data present the electrowetting forces.

6. Results and Discussion

The pumping technique presented is tested experimentally. An AC square wave signal with the frequency of $f = 1 \text{ kHz}$ and amplitude in the range of $100\text{--}200 \text{ V}_{p-p}$ is applied for manipulation of the piston droplet on the array of the copper electrodes. Fig. 6 presents the schematic of the setup and the procedure followed for turning the electrodes on and off to actuate the droplet back and forth in the microchannel. It is observed that the shape of the pumped droplet during pumping does not change. Thus, the velocity profile of the pumped liquid can be assumed as a plug-flow velocity profile.

Fig. 7 presents the displacement of the pumped droplet as a function of the applied voltage. In essence, an increase in the actuation voltage

amplifies the displacement of the droplet. However, after a certain voltage value (150 volts) the displacement of the pumped liquid becomes independent of the voltage and just dependent on the actuation period of the actuation signal (t_{on}) (see Fig. 7). Using the described signal modulation technique, t_{on} can be precisely controlled. This way, the power consumption of the entire system decreases dramatically, as the actuation signal is only applied for a short period (it is turned off using the designed interface circuit for a long time (t_{off}) compared to the turned-on period (t_{on})).

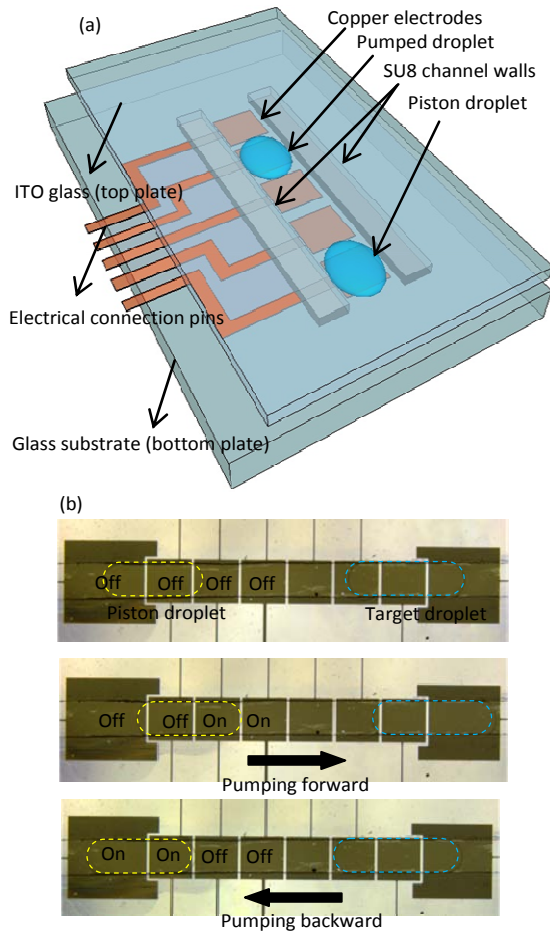


Fig. 6. (a) Schematic of the fabricated device, (b) pumping a droplet back and forth in a microchannel integrated on a DMF platform.

By applying the on/off signal frequently, the piston droplet is manipulated with nearly a constant velocity in the channel. As a result, the pumped droplet is driven in the channel with the same velocity as that of the piston droplet. The average velocity of the pumped droplet is shown in Fig. 8 for three different cases in the SU8 microchannel design.

Different flow rates of the pumped liquid can be achieved by precisely controlling t_{on} of the applied voltage (the flow rate is equal to the cross sectional area of the microchannel multiply by the average velocity presented in Fig. 8). Due to the fact that the

velocity profile of the liquid after the pumped droplet is uniform (which means the plug flow is observed), the flow rate of the liquid after the pumped droplet is directly proportional to the pumped droplet velocity. As a result, a controlled flow rate of the liquid in the channel is achieved by the presented technique. Although the displacement of the liquid is dependent on the gap size (d), it is also possible to change the average flow rate of the fluid in the microchannel by changing t_{off} and keeping t_{on} constant (which means that similar scenario can be used for the 3D-printed design to create desired pumping flow rates).

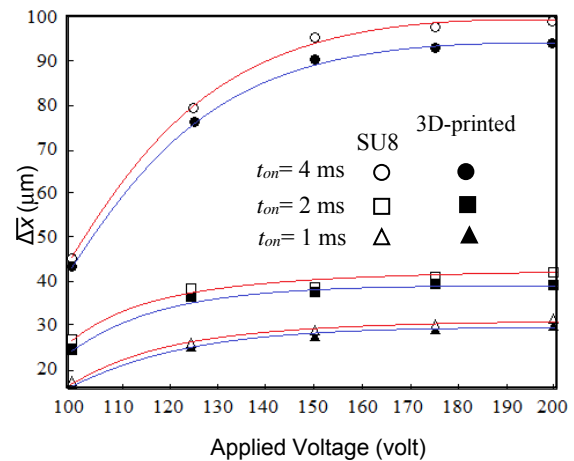


Fig. 7. Droplet average displacement vs. the voltage amplitude (V_{pp}). Three different t_{on} were tested (shown with different symbols) for two different microchannel designs: SU8-based (red lines) and 3D-printed (blue lines) microchannels.

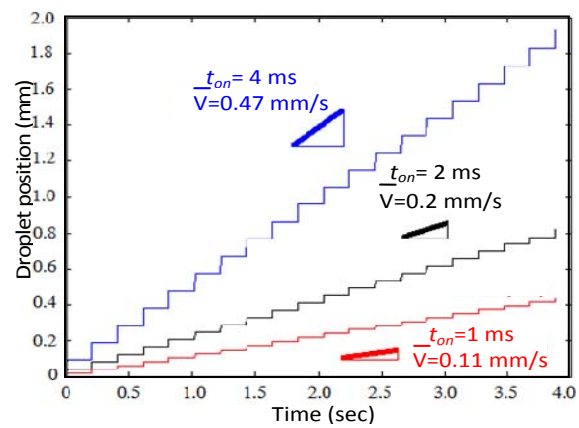


Fig. 8. The position of the pumped liquid using the pulse modulation technique.

7. Conclusions


Manipulation of a column of liquid in a microchannel integrated on a DMF platform is achieved using two different methods of fabrication of the microchannel. A target droplet is pumped into the microchannel using the moving force of a

secondary droplet, which is actuated using EWOD on an array of electrodes. It is observed that the shape of the pumped droplet during pumping does not change which suggests that the velocity profile of the pumped liquid be a plug-flow. A signal modulation technique is developed and used in order to control the flow rate of the liquid column in the microchannel and to lower the power consumption of the microfluidic system. Different flow rates of the pumped liquid are created by precisely controlling the actuation time (t_{on}) of the signal used for actuation the piston droplet.

References

- [1]. P. Neuzil, C. D. M. Campos, C. C. Wong, W. S. Bo, J. Reboud, A. Manz, From chip-in-a-lab to lab-on-a-chip: towards a single handheld electronic system for multiple application-specific lab-on-a-chip (ASLOC), *Lab Chip*, Vol. 14, Issue 13, 2014, pp. 2168-2176.
- [2]. M. J. Cooper, G. M. Whitesides, Poly (dimethylsiloxane) as a material for fabricating microfluidic devices, *Accounts of Chemical Research*, Vol. 35, Issue 7, 2002, pp. 491-499.
- [3]. K. Dholakia, P. Reece, M. Gu, Optical micromanipulation, *Chemical Society Reviews*, Vol. 37, Issue 1, 2008, pp. 42-55.
- [4]. K. R. Balakrishnan, G. Anwar, M. R. Chapman, T. Nguyen, A. Kesavaraju, L. L. Sohn, Node-pore sensing: a robust, high-dynamic range method for detecting biological species, *Lab Chip*, Vol. 13, Issue 7, 2013, pp. 1302-1307.
- [5]. F. Hossein-Babaei, M. Paknahad, V. Ghafarinia, A miniature gas analyzer made by integrating a chemoresistor with a microchannel, *Lab Chip*, Vol. 12, Issue 10, 2012, pp. 1874-1880.
- [6]. J. Castillo, M. Dimaki, W. E. Svendsen, Manipulation of biological samples using micro and nano techniques, *Integr. Biol.*, Vol. 1, Issue 1, 2009, pp. 30-42.
- [7]. R. B. Fair, Digital microfluidics: is a true lab-on-a-chip possible ?, *Microfluidics and Nanofluidics*, Vol. 3, Issue 3, 2007, pp. 245-281.
- [8]. H. Rezaei Nejad, M. Hoorfar, Purification of a droplet using negative dielectrophoresis traps in digital microfluidics, *Microfluidics and Nanofluidics*, June 2014.
- [9]. M. J. Jebrail, M. S. Bartsch, K. D. Patel, Digital microfluidics: a versatile tool for applications in chemistry, biology and medicine, *Lab Chip*, Vol. 12, 2012, pp. 2452-2463.
- [10]. H. Rezaei Nejad, O. Z. Chawdhury, M. D. Buat, M. Hoorfar, Characterization of the geometry of negative dielectrophoresis traps for particle immobilization in digital microfluidic platforms, *Lab Chip*, Vol. 13, Issue 9, 2013, pp. 1823-1830.
- [11]. H. Rezaei Nejad, M. Paknahad, M. Hoorfar, Introducing a Digital Micropump for Driving a Droplet in a Microfluidic Channel, in *Proceedings of the Conference 'TechConnect World'14*, Washington DC, United States, 15-18 June 2014.

2014 Copyright ©, International Frequency Sensor Association (IFSA) Publishing, S. L. All rights reserved.
(<http://www.sensorsportal.com>)




Smart Sensors and MEMS

Edited by
**Sergey Y. Yurish and
Maria Teresa S.R. Gomes**

The book provides a unique collection of contributions on latest achievements in sensors area and technologies that have made by eleven internationally recognized leading experts ...and gives an excellent opportunity to provide a systematic, in-depth treatment of the new and rapidly developing field of smart sensors and MEMS.

The volume is an excellent guide for practicing engineers, researchers and students interested in this crucial aspect of actual smart sensor design.



Kluwer Academic Publishers

Order online: www.sensorsportal.com/HTML/BOOKSTORE/Smart_Sensors_and_MEMS.htm